

Fast Correction Method for Abdominal Multi-Organ Segmentation Using 2D/3D Free Form Deformation and Posterior Shape Models

Waldo Valenzuela¹ *, Juan Cerrolaza², Ronald M. Summers³, Marius George Linguraru², and Mauricio Reyes¹

¹ Institute for Surgical Technology and Biomechanics, University of Bern, Switzerland

² Sheikh Zayed Institute for Pediatric Surgical Innovation, Children’s National Medical Center, Washington DC 20010, United States

³ National Institutes of Health, Bethesda, Maryland, United States

Abstract. Despite advances in automatic medical image segmentation, time-effective interactive correction tools are commonly required in the clinical environment. In this work we present a new interactive correction method for abdominal multi-organ segmentation. Our method enables 3D shape corrections through 2D interactions. During runtime local corrections are used to build a conditional model, which infers the shape of neighboring organs. The combination of 2D/3D shape deformation model with a mechanism to propagate local corrections enables an intuitive and natural manipulation of 3D segmentation results, and reduces substantially the number of interactions and correction time used for multi-organ correction. Experimental results show the ability of the proposed approach to produce high quality segmentations with 82% and 57% reductions on the number of user interactions and correction time, respectively, in comparison to corrections performed on a single-organ basis.

1 Introduction

The wide variability of imaging protocols, scanning parameters, and the intrinsic discrete nature of medical imaging devices, makes image segmentation a difficult task [1]. In clinical radiological evaluation of abdominal disorders this difficulty is further increased, as the clinical diagnosis does not rely solely on the analysis of a single organ, but on a comprehensive analysis over a group of organs [2]. Therefore, the segmentation task becomes a multi-organ problem. From the early 1980’s, these problems have been addressed from a variety of directions [1, 3, 4]. Pattern recognition, image processing, and computer vision fields have assembled a wide spectrum of segmentation algorithms. Nevertheless, the performance of these algorithms is still application-specific and despite the progress in automatic segmentations, the segmentation task has become in practice a process where

* waldo.valenzuela@istb.unibe.ch

a post-correction and checking of the segmentation result has to be performed in order to obtain accurate results of clinical utility. Nowadays the corrections methods used in the clinics are still performed on a single organ basis, and the most popular correction methods employed are still two-dimensional (e.g. brushing, active 2D-contours, manual polygons). Clinicians (typically a radiologist) spend exhaustive time checking slice by slice, and correcting segmentation results using these tools. In this regard, it is essential to reduce the correction time while maintaining and improving the quality of the final segmentation with minimal number of interactions.

Several correction methods have been proposed in the literature, e. g., Heckel et al. [5] used a 2D live-wire extrapolation to edit the segmentation contours, Grady et al. [6] employed a graph approach to edit the initial segmentation, and Kronman et al. [7] applied a combination of min-cut segmentation and laplacian deformation for the correction. Criminisi et al. [8] created a segmentation tool (GeoS) based on a conditional random field and geodesic distance, which also could be used for segmentation correction through refining of the segmentation via additional brushes enforcing corrections or by slice-wise 2D brushing techniques. These corrections tools are suitable to correct errors from algorithms based on image thresholding or pattern recognition techniques. However, algorithms based on deformable models, where the error is caused by the initial alignment or the registration technique [9], would need other approach. In [10], Schwarz et al. proposed the use of contour-dragging interactions and a Gaussian kernel in order to weigh the local influence of 3D shape deformations. In [11], Timinger et al. proposed a modified active shape model-based segmentation that introduces user interactions into a user-defined deformation energy term. In these **single-organ correction approaches** special attention is needed in order to correctly define the size of the Gaussian kernel used to locally weigh user-based deformations.

In this paper, we present, to the best of our knowledge, the first multi-organ correction method, which focused on reducing the correction time and the number of interactions of multi-organ segmentation. Our approach produces real-time 3D multi-organ correction through 2D contour manipulation over the initial segmentation. Inspired by the 3D direct manipulation approach presented by Hsu et al. [12] where the Free Form Deformation (FFD) of Sederberg et al. [13] was improved. We created a new intuitive 2D/3D shape manipulation tool oriented to clinical environment. The correction result, produced by these CAD techniques, is used to build a posterior statistical shape model [14, 15] to infer the shape of neighbouring organs. In this way, user corrections performed at the organ level can be effectively propagated to neighbouring organs, enabling in this way a **faster and intuitive multi-organ segmentation correction**.

We demonstrate the ability of the proposed approach to yield a substantial correction speed-up on segmentations produced with the recently proposed Generalized Hierarchical Active Shape Model [16]. On a set of leave-one-out experiments on a database of 18 abdominal CT images comprising spleen, right and left kidneys, gallbladder, pancreas, liver and stomach, we demonstrate the

ability of the proposed approach to produce high quality segmentations with an average of 82% reduction on the number of user interactions, and a 57% reduction on the correction time, as compared to the single-organ based method. Similarly, at the same number of interactions the proposed approach yields an average increase in Dice coefficient of 26.3%.

2 Methods

The proposed correction method is shown in Figure 1. As inputs an initial segmentation and the corresponding medical image are loaded into the system. Three 2D views (sagittal, coronal and axial) with the overlaid contour of the 3D segmented shape are displayed. These contours are created from the intersection between the slice planes and the 3D shape. The correction process is performed through contour manipulation, where the user can drag and drop any point of the contour. After the mouse drop event is triggered, the deformation method (section 2.1) updates the shape based on the desired position. This new shape is used in conjunction with a shape model of the organs to build a posterior shape model, which will update the shape of neighbouring organs (section 2.2). Finally, the 2D slices with the new contours are automatically updated in real-time, enabling a fluent correction process. In the following sections we describe in details each part of the correction pipeline.

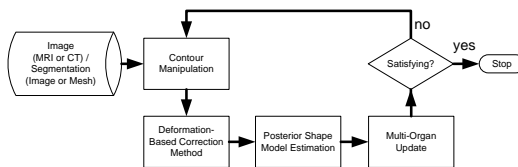


Fig. 1: Correction Pipeline. As inputs, the system receives a medical image and the segmentation result (labeled image or mesh). The correction is performed through contour manipulation in a 2D environment, this manipulation is then transformed to a 3D shape deformation, which is then used within a statistical shape model scheme to create a posterior model that predicts the shape of neighbouring organs. This process continues over several iterations until the user is satisfied with the final result.

2.1 Deformation-Based Correction Method: from 2D interactions to organ-level corrections

To create a fast and intuitive interactive correction framework, we propose a FFD [13] based model to generate 3D deformations from 2D user interactions. In particular, the proposed model is deformed in terms of a tensor product of trivariate Bezier polynomial. The new shape of the geometrical model \mathbf{X} can be computed as

$$x_{ffd} = \sum_{i=0}^l \binom{l}{i} \left[(1-s)^{l-i} s^i \left[\sum_{j=0}^m \binom{m}{j} (1-t)^{m-j} t^j \left[\sum_{k=0}^n \binom{n}{k} (1-u)^{n-k} u^k \mathbf{P}_{ijk} \right] \right] \right] \quad (1)$$

, where x_{ffd} is the deformed position of the point x , \mathbf{P} is a vector containing the Cartesian coordinates of the control points created on the parallelepiped region of \mathbf{X} (see white grid in Figure 2), and (s, t, u) are the coordinates of the point x in terms of the local coordinate system. Thanks to this mathematical model (Eq. (1)), the user is able to control the 3D deformation process through 3D control points manipulation. However, the direction of the movement of the control points is not directly related to the desired deformation (i.e. the user has to figure out the position of the control point that yields a specific deformation of the mesh). To solve this issue, and thus enable direct 3D deformations from contour manipulations, we adopted the Direct-Manipulation of FFD model proposed by Hsu et al [12] where a direct manipulation on the mesh is performed by the user, which will be used to compute the position of the control points that produce such deformation.

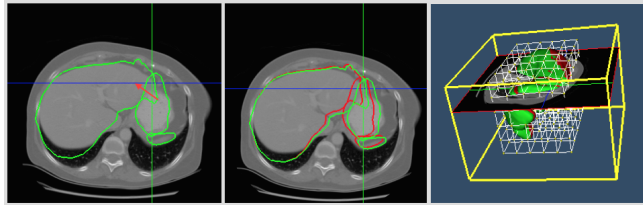


Fig. 2: Overlapping challenge. Left: Red arrow shows the direction of the correction needed to solve the overlapping between the liver and the stomach. Center: after correction, both organs move in the same direction and the overlapping remains. Right: Grid of control point covering all the organs.

2.2 Posterior Shape Model Estimation: from organ-level to multi-organ corrections

The corrected organ, produced by the deformation model presented in section 2.1 can be combined with an existing statistical shape model of the abdominal organs (e.g. [16, 2]) to build a posterior shape model [14, 15] of the abdominal organs. The main idea is to influence the shape of neighbouring organs by the shape of corrected organ \mathbf{s}_g . The hypothesis is that the shape correlation among organs enables improved shape predictions of these neighbouring organs [16]. Formally, given a statistical shape model as a multivariate normal distribution $\mathcal{N}(\boldsymbol{\mu}, \boldsymbol{\sigma})$, a principal component analysis of the covariance matrix ($\boldsymbol{\sigma} = \mathbf{U}\mathbf{D}^2\mathbf{U}^T$) enables a compact parametric representation of shapes $\mathbf{s}(\boldsymbol{\alpha}) = \boldsymbol{\mu} + \mathbf{U}\mathbf{D}\boldsymbol{\alpha} = \boldsymbol{\mu} + \mathbf{Q}\boldsymbol{\alpha}$. Given a partial or complete corrected organ shape, a posterior shape model $\mathcal{N}(\boldsymbol{\mu}_c, \boldsymbol{\sigma}_c)$ can be computed as,

$$\begin{aligned} p(\mathbf{s}|\mathbf{s}_g) &= \mathcal{N}(\boldsymbol{\mu} + \mathbf{Q}\boldsymbol{\eta}, \mathbf{Q}\boldsymbol{\Lambda}\mathbf{Q}^T) \\ \boldsymbol{\mu}_c &= \boldsymbol{\mu} + \mathbf{Q}(\mathbf{Q}_g^T\mathbf{Q}_g + \sigma^2\mathbf{I}_n)^{-1}\mathbf{Q}_g^T(\mathbf{s}_g - \boldsymbol{\mu}_g) \\ \boldsymbol{\Sigma}_c &= \sigma^2\mathbf{Q}(\mathbf{Q}_g^T\mathbf{Q}_g + \sigma^2\mathbf{I}_n)^{-1}\mathbf{Q}^T, \end{aligned} \quad (2)$$

with $\boldsymbol{\eta} = (\mathbf{Q}_g^T\mathbf{Q}_g + \sigma\mathbf{I}_n)^{-1}\mathbf{Q}^T(\mathbf{s}_g - \boldsymbol{\mu}_g)$, \mathbf{I}_n a shrinkage term used for covariance estimation, and \mathbf{Q}_g and $\boldsymbol{\mu}_g$ submatrices of \mathbf{Q} and $\boldsymbol{\mu}$ corresponding to

the corrected organ, respectively. The resulting posterior distribution, $p(\mathbf{s}|\mathbf{s}_g)$ is then modeled by the posterior mean $\boldsymbol{\mu}_c$ and posterior covariance $\boldsymbol{\Sigma}_c$.

After the posterior model is created, the posterior mean $\boldsymbol{\mu}_c$ represents the most likely shape given the partial data. In this way, the corrections performed on the specific organ is propagated to the neighbouring organs. Furthermore, this will also solve the common overlapping problem present on multi-organ segmentation result, Figure 2. Although, this problem could be solved using the deformable model on a single-organ basis, this would be time-consuming, as we will show on the results section. In addition, in the results section we demonstrate how a cascade of corrections and posterior shape models can be used to exploit studied shape correlations among abdominal organs [2]. Based on the findings of Okada et. al [2] we followed the cascaded correction protocol as follows (the right arrow indicates the order by which the corrections take place), Liver→Spleen→Pancreas→Gallbladder→Right Kidney→Left Kidney→Stomach (the Stomach was not included in Okada study, hence we include it at the end of the cascade correction). Upon user corrections the corrected organ shape is “frozen” and kept fix for the following levels of the cascade. The posterior component of the statistical shape model is then augmented with the corrected organ in order to further add information to the organ to be corrected next.

3 Results

In order to test the performance of the proposed correction method by an expert user, we developed a GUI software tool⁴. We used the Insight Toolkit for Segmentation and Registration (ITK, <http://www.itk.org>), and the visualization Toolkit (VTK, <http://www.vtk.org>) with Qt (<http://qt-project.org>) for visualization and GUI. To create the Statistical Shape Model (SSM) and the Posterior Shape Model we used the Statismo framework [17]. To quantify results, the software records the number of interactions performed by the user, with a single interaction defined as a “*mouse-down-mouse-up*” event on the GUI viewer.

3.1 Data and experiments

We used a proprietary dataset of 18 CT abdominal patient images (High resolution scan with 1 mm slice thickness and in-slice resolution from 0.54 mm to 0.91 mm), with each case comprising seven organs (spleen, left and right kidney, gallbladder, pancreas, liver, and stomach). Each organ was manually segmented under the supervision of a board certified radiologist to generate a ground-truth segmentation. As metrics we used Dice coefficient and recorded the number of interactions. As input segmentations to be corrected we used segmentations generated by the approach recently proposed by Cerrolaza et al. [16], where a Generalized-Hierarchical Active Shape Model (*GH-ASM*) was used for multi-organ abdomen segmentation.

⁴ Software video: <https://www.youtube.com/watch?v=BV6Eixd5nso>

Two experiments were designed to evaluate the correction speed and quality of both, the Single-Organ Free Form Deformation model, termed below *SO-FFD*, and of the Multi-Organ posterior shape model Free Form Deformation approach, termed below *MO-FFD*.

Experiment 1: Single-organ correction. The aim of this first experiment was to quantify the number of interactions and the correction time needed to perform a correction of the complete set of organs using *SO-FFD*. Each organ was corrected individually and the total number of corrections was recorded. The stopping criteria for the correction was defined qualitatively by the expert user, as the point where an adequate contour matching was obtained for the entire organ. In addition, corrections were stopped when the user identified no possible further improvements. We remark that definition of a given Dice coefficient as stopping criteria was not used as the quality of the segmentations vary from organ to organ, making the definition of a single value difficult. We also emphasise that the goal of these experiments is not to outperform previous methods in terms of dice, but to demonstrate improved results at a lower number of user interactions. As shown in Figure 3, 300 interactions were needed to increase the initial average Dice coefficient from 0.75 ± 0.12 to 0.91 ± 0.1 . A total time of 70 ± 10 minutes of correction time per set of organs was required.

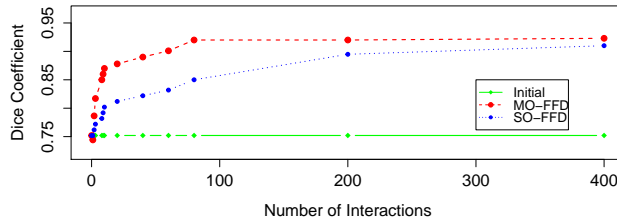


Fig. 3: Average correction accuracy. These curves shows the average Dice coefficient of seven organs of the abdominal region. Correction using *MO-FFD* (blue curve), the red curve correction using *SO-FFD* method.

Experiment 2: Multi-organ correction. In this second experiment we evaluated the ability of the proposed *MO-FFD*, to yield faster and improved corrections of the organs. The analysis focused at the organ level in order to better understand the behaviour of the method using a cascading correction scheme, presented below. In these experiments we use a leave-one-out scheme to create the input segmentations [16] and the posterior shape model. Figure 3 summarizes results for both *SO-FFD* and *MO-FFD*. Although we do not report the results herein, *SO-FFD* yields a sixfold speedup as compared to the common slice-by-slice manual segmentation approach used in the clinics. Moreover, as shown in Figure 3, *MO-FFD* delivers much faster corrections than *SO-FFD*. Only 54 interactions were needed to reach an average Dice coefficient of 0.9 ± 0.05 , which is reflected on the reduction of the correction time by 57% (30 ± 2 minutes per case).

Table 1: Dice Coefficient per Organ. The first row is the initial Dice coefficient with segmentation ASM-based. The second row shows the final dice after correction.

	Liver	Spleen	Pancreas	Gallbladder	Right Kidney	Left Kidney	Stomach
Initial Dice	0.863	0.847	0.672	0.738	0.814	0.512	0.817
Final Dice	0.886 (+3%)	0.880 (+4%)	0.862 (+28%)	0.890 (+21%)	0.948 (+17%)	0.938 (+83%)	0.901 (+10%)

In Table 1 we report initial ([16]) and final Dice coefficient values after *MO-FFD* for each organ. From Table 1, it can be concluded that the proposed methodology increase on an average of 23.3% the initial segmentation with 57% of reduction in the correction time from a single-organ approach. Noteworthy that we used the same grid resolution for all the organs corrected. In future work we will include adaptive resolution, to improve the correction accuracy of FFD on organs like the liver that has a high shape complexity. In organs such that spleen, where the correction was mostly driven by the posterior shape model, an improvement on the accuracy could be achieved through an increased number of interactions. Also, the combination of the cascade model together with FFD correction enabled a significant increase of speed and accuracy on organs that are difficult to segment (pancreas, gallbladder and stomach).

4 Discussion and Conclusions

The variety of image protocols and the quality of radiological images has shown to produce errors in the result of segmentation algorithms. Therefore, correction of image segmentation results is a common and crucial step for clinical analysis. Specially in clinical radiology of abdominal organs where a fast and robust multi-organ segmentation correction is needed for an effective clinical workflow and diagnosis.

In this work we present a new interactive correction method for multi-organ segmentation. Our method provides a 2D/3D environment that enables 3D shape corrections through simple 2D interactions. During runtime, local corrections are combined with a statistical shape model to build a conditional model, which when used in a cascading scheme of known inter-organ correlations, allows us to effectively infer the shape of neighbouring organs. The combination of a 2D/3D shape deformation model with a mechanism to propagate local corrections enables an intuitive and natural manipulation of 3D segmentation results, and reduces substantially the number of interactions used for multi-organ correction. The proposed method provides a natural and real time user-interface for correction of 3D medical image segmentations that has the potential to be incorporated in the clinical environment.

Experimental results on a database of abdominal organs (spleen, kidneys, gallbladder, pancreas, liver and stomach) show the ability of the proposed approach to produce high quality segmentations with a 82% reduction on the number of user interactions, as compared to the number of interactions performed on a single-organ basis. Similarly, with the same number of interactions the proposed approach yields an average increase of Dice coefficient of 26.3%, with a

reduction of the correction time of 57% in comparison to the single-organ approach. Future work includes the notion of segmentation quality assessment, which can be learned from existing data or through previously proposed assessment metrics, in order to pre-evaluate the input segmentation at a local and organ-base level, and with this enabling improved multiple-organ corrections.

5 Acknowledgments

This research was supported partly by the intramural research program of the National Institutes of Health, Clinical Center, and by AOSpine International.

References

1. Duncan, J., et al.: Medical image analysis: Progress over two decades and the challenges ahead. *IEEE-TPAMI* **22**(1) (2000) 85–106
2. Okada, T., et al.: Multi-organ segmentation in abdominal CT images. *EMBS* (2012) 3986–3989
3. Linguraru, M., et al.: Multi-organ segmentation from multi-phase abdominal CT via 4D graphs using enhancement, shape and location optimization. *Lecture Notes in Computer Science* (2010) 89–96
4. Selver, M.A.: Segmentation of abdominal organs from CT using a multi-level, hierarchical neural network strategy. *CMPB* **113**(3) (2014) 830–852
5. Heckel, F., et al.: Sketch-based Image-independent Editing of 3D Tumor Segmentations using Variational Interpolation. *EWVCBM* (2012) 73 – 80
6. Grady, L., Funka-Lea, G.: An energy minimization approach to the data driven editing of presegmented images/volumes. *MICCAI* **9**(Pt 2) (January 2006) 888–95
7. Kronman, A., Joskowicz, L.: Image Segmentation Error Correction by Mesh Segmentation and Deformation. *MICCAI* (2013) 206–213
8. Criminisi, A., Sharp, T., Blake, A.: GeoS: Geodesic image segmentation. *Lecture Notes in Computer Science* **5302 LNCS**(PART 1) (2008) 99–112
9. Heimann, T., Meinzer, H.P.: Statistical shape models for 3D medical image segmentation: a review. *Medical image analysis* **13**(4) (August 2009) 543–63
10. Schwarz, T., et al.: Interactive Surface Correction for 3D Shape Based Segmentation. *Proceedings of SPIE* **6914** (March 2008) 69143O–69143O–8
11. Timinger, H., Pekar, V., von Berg, J.: Integration of Interactive Corrections to Model-Based Segmentation Algorithms. (2003) 171 –175
12. Hsu, W., Hughes, J., Kaufman, H.: Direct manipulation of free-form deformations. *ACM Siggraph Computer Graphics* **2**(July) (1992) 177–184
13. Sederberg, T., Parry, S.: Free-Form Deformation of Solid Geometric Models. *ACM Siggraph Computer Graphics* **20**(4) (1986) 151–160
14. Albrecht, T., et al.: Posterior shape models. *Medical Image Analysis* **17**(8) (2013) 959–973
15. Blanc, R., et al.: Statistical model based shape prediction from a combination of direct observations and various surrogates: application to orthopaedic research. *Medical image analysis* **16**(6) (August 2012) 1156–66
16. Cerrolaza, J.J.: Generalized Multiresolution Hierarchical Shape Models via Automatic Landmark Clusterization. In: *MICCAI*. (2014)
17. Luthi, M., et al.: Statismo-A framework for PCA based statistical models. *The Insight Journal* (2012) 1–18